Effect of the Anchoring Group (Carboxylate vs Phosphonate) in Ru-Complex-Sensitized TiO$_2$ on Hydrogen Production under Visible Light

Eunyoung Bae and Wonyong Choi*

School of Environmental Science and Engineering, Pohang University of Science and Technology (POSTECH), Pohang 790-784, Korea

We synthesized six Ru−bipyridyl complexes having di-, tetra-, and hexacarboxylate (**C2**, **C4**, and **C6**) and di-, tetra-, and hexaphosphonate (**P2**, **P4**, and **P6**) as the anchoring group, prepared six different sensitized TiO$_2$ samples by using them, and then systematically tested their visible light reactivity for hydrogen production in aqueous suspension (with EDTA as an electron donor) under $\lambda > 420$ nm illumination. The properties and efficiencies of C- and P-complexes as a sensitizer depended on the number and kind of anchoring groups in very different ways. The adsorption of P-complexes on TiO$_2$ is strong enough not to be hampered by the presence of competing adsorbates (EDTA), whereas that of C-complexes is significantly inhibited. As a result, P−TiO$_2$ exhibited much higher activity for the hydrogen production than C−TiO$_2$, although the visible light absorbing capabilities are comparable among C- and P-complexes. Among the six sensitizers, **P2** was the most active one for the H$_2$ production. The hydrogen production activities of C−TiO$_2$ and P−TiO$_2$ depended on the concentration of sensitizers and electron donors in different ways as well. How the sensitizing activity for hydrogen production is influenced by the anchoring group and the experimental conditions was investigated and discussed in detail. It is also notable that the effects of the anchoring group on the sensitized production of hydrogen were drastically different from those on the dye-sensitized solar cell we recently reported for the same set of six sensitizers.

Introduction

Photocatalytic hydrogen production has been a challenging issue for decades for the realization of hydrogen economy.[1−9] Many active photocatalysts that split water into hydrogen and oxygen under UV irradiation have been reported, but the visible light active materials for practical applications remain to be developed.[5−9] The visible light active photocatalysts under development can be divided into two categories: (1) modified wide band gap oxide semiconductors (e.g., TiO$_2$ doped by impurities or sensitized by dyes)[10−15] and (2) new composite materials with complex structure.[8,9,16−18]

TiO$_2$ has been one of the most popular photocatalysts, but its inactivity in the visible light region limits its practical applications. Dye sensitization of TiO$_2$ has been extensively studied as a mean of visible light activation,[19−24] which has been very successful in dye-sensitized solar cells (DSSCs).[25−29] Dye molecules attached on the TiO$_2$ surface are excited by absorbing visible light and subsequently inject electrons into the conduction band (CB) of TiO$_2$ to generate photocurrent through an external circuit (in DSSCs) or to initiate an interfacial chemical reaction (in sensitized conversion). We have previously reported that TiO$_2$ particles sensitized by ruthenium bipyridyl complexes (RuL$_x$) degraded perchloro compounds (e.g., CCl$_4$ and trichloroacetate) in a reductive path.[21,22] The visible light induced production of hydrogen on sensitized TiO$_2$ is based on the same principle, which is briefly illustrated in Scheme 1. However, the great success of the ruthenium-complex-sensitized TiO$_2$ in DSSCs is sharply contrasted with its much reduced popularity in photocatalysis, which is largely ascribed to the

SCHEME 1: Illustration of Visible Light Induced H$_2$ Production on a Ruthenium-Complex-Sensitized TiO$_2$ Particle in Water^a
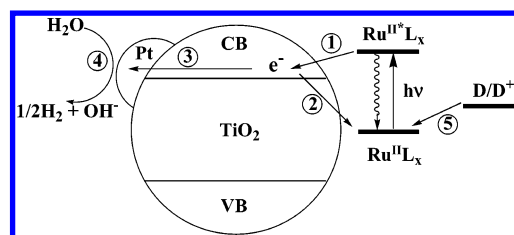
^{a} The number represents the major electron pathways: 1, electron injection from the excited sensitizer to CB; 2, back-electron-transfer to the oxidized sensitizer (Ru^{III}L$_x$); 3, electron migration and trapping in Pt deposits; 4, interfacial electron transfer to H$_2$O (or H$^+$) on Pt; 5, sensitizer regeneration by an electron donor (D) (EDTA in this case).

inefficiency and instability of the sensitizers anchored onto TiO$_2$ in aquatic environments. RuL$_x$ is usually anchored onto the surface of TiO$_2$ through carboxylate linkages that are intrinsically vulnerable to hydrolytic cleavage. An alternative anchoring group such as phosphonate has been found to be often more effective and stable in RuL$_x$-sensitized electrode or photocatalysis.[30−35] In this respect, the effects of anchoring groups in RuL$_x$ on the overall sensitization performance need to be understood in detail. In a recent study,[36] we have synthesized six RuL$_x$ sensitizers having di-, tetra-, and hexacarboxylate (**C2**, **C4**, and **C6**) and di-, tetra-, and hexaphosphonate (**P2**, **P4**, and **P6**) as the anchoring groups and compared their binding to TiO$_2$ surface and their photoelectrochemical performance in DSSCs. Their surface binding on TiO$_2$ and the overall cell performance were highly dependent on both the number and the kind of

* Corresponding author. E-mail: wchoi@postech.ac.kr.

anchoring groups. Among them, we have found that **C4**- and **P6**-sensitized TiO$_2$ photoelectrodes showed the best cell performance.

This study extends our previous investigation on the anchoring group effect to the sensitized production of hydrogen in the RuL$_x$/TiO$_2$ system. The hydrogen production efficiency was also highly influenced by the kind of anchoring group, but the anchoring group effects were markedly different from those in DSSC. The relation between the anchoring-group-dependent properties and the hydrogen production activities is investigated and discussed in detail.

Experimental Section

Sensitizer Preparation and Characterization. [Ru(bpy)$_2$-(4,4′-dicarboxy-2,2′-bipyridine)](PF$_6$)$_2$ (**C2**), [Ru(bpy)(4,4′-dicarboxy-2,2′-bipyridine)$_2$bpy]$_2$(PF$_6$)$_2$ (**C4**), [Ru(4,4′-dicarboxy-2,2′-bipyridine)$_3$]Cl$_2$ (**C6**), [Ru(bpy)$_2$(4,4′-(PO$_3$H$_2$)$_2$bpy)]Br$_2$ (**P2**), [Ru(bpy)(4,4′-(PO$_3$H$_2$)$_2$bpy)$_2$](PF$_6$)$_2$ (**P4**), and [Ru(4,4′-(PO$_3$H$_2$)$_2$-bpy)$_3$](PF$_6$)$_2$ (**P6**) were synthesized and used as sensitizers of TiO$_2$ (bpy is 2,2′-bipyridine). Their structures are shown below.
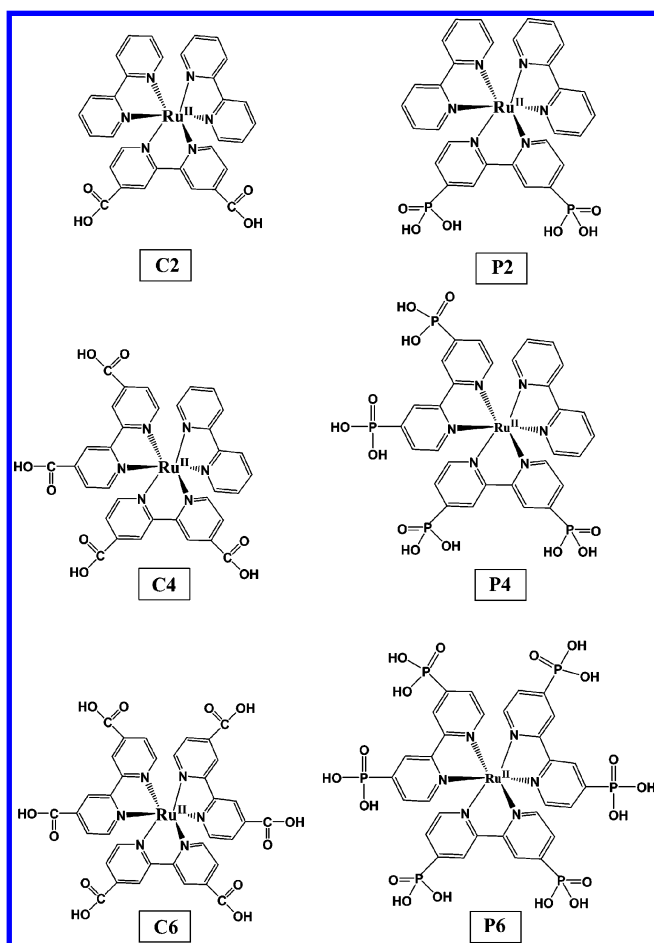
Six sensitizers were prepared by following literature methods. **C2**, **C6**, and **P2** were available from our previous studies.[21,22] **C4** was synthesized through reacting RuCl$_3$ with 4,4′-dicarboxy-2,2′-bipyridine (60% yield).[37] **P4** was synthesized through a two-step route: starting from RuCl$_3$ and 4,4′-diethyl phosphonato-2,2′-bipyridine[38] and finally to [Ru(bpy)(4,4′-(PO$_3$H$_2$)$_2$bpy)$_2$](PF$_6$)$_2$ (15% yield).[39] **P6** was obtained by the reaction of RuCl$_3$ with 4,4′-diethyl phosphonato-2,2′-bipyridine (40% yield). Removing free bipyridyl ligands through precipitation and recrystallization purified the synthesized ruthenium complex samples. The detailed synthetic procedures and the characterization results

of the six complexes can be found in our recent paper.[36] The six sensitizers are all dissolved in water.

A UV–vis spectrophotometer (Agilent 8453) was used for the analysis of the sensitizers. The absorption spectra of these complexes show typical characteristics of the ruthenium bipyridyl complexes with an intense UV band (∼300 nm), assigned to ligand-centered $\pi \rightarrow \pi^*$ transitions, and a broad band in the visible region, due to metal-to-ligand charge-transfer (MLCT) transitions (d → π^*).[33] The maximum of the MLCT band (at pH 3 in water) is located at λ_{max} of 457, 472, 467 nm for **C2**, **C4**, and **C6** and 456, 488, and 464 nm for **P2**, **P4**, and **P6**, respectively (see Supporting Information for spectra). The molar absorptivities of **C2**, **C4**, and **C6** were determined to be 1.6 × 10^4, 1.0 × 10^4, and 1.9 × 10^4 M^{-1} cm^{-1}; those of **P2**, **P4**, and **P6** were 1.0 × 10^4, 7.7 × 10^3, and 2.4 × 10^4 M^{-1} cm^{-1}, respectively. They were used in determining the concentration of the sensitizer. The fluorescence emission spectra of C-series and P-series complexes in water were obtained with a spectrofluorometer (Shimadzu RF-5301). The MLCT emission (λ_{ex} = 460 nm) maxima of six sensitizers are 645, 637, and 628 nm for **C2**, **C4**, and **C6** and 623, 619, and 606 nm for **P2**, **P4**, and **P6**, respectively (see Supporting Information for spectra). **C6** and **P6** have higher absorption and emission in the visible region than the other sensitizers with fewer anchoring groups. **C4** and **P4** are peculiar in that their MLCT bands have the lowest absorptivities and the lowest emission intensity. In particular, **P4** is very weak in the visible light absorption and almost completely inactive for the emission.

Chemicals. TiO$_2$ (Degussa P25), a mixture of 80% anatase and 20% rutile with an average surface area of 50 ± 15 m^2/g, was used as a main support of the sensitizers. Three other commercial TiO$_2$ samples (Ihihara ST-01, Hombikat UV-100, and Aldrich anatase) were also compared for their activity for the sensitized hydrogen production. Chloroplatinic acid (H$_2$-PtCl$_6$·6H$_2$O) (Aldrich) and ethylenediaminetetraacetic acid (EDTA, Aldrich) were used as received as a precursor of Pt deposition on TiO$_2$ and a sacrificial electron donor, respectively. Deionized water used was ultrapure (18 MΩ·cm) and prepared by a Barnstead purification system.

Photocatalyst Preparation and Characterization. Platinum nanoparticles were loaded onto TiO$_2$ particles using a photodeposition method. The platinization was carried out in an aqueous suspension of TiO$_2$ (0.5 g/L) in the presence of 1 M methanol (electron donor) and 1 × 10^{-4} M chloroplatinic acid (H$_2$PtCl$_6$) under UV irradiation for 30 min (with a 200-W mercury lamp). After irradiation, the Pt/TiO$_2$ powder was filtered and washed with distilled water. A typical Pt loading on TiO$_2$ was estimated to be ca. 3 wt % by comparing the platinum concentrations before and after the photodeposition. Transmission electron microscopic images of Pt/TiO$_2$ showed Pt particles with a size range of 1−4 nm dispersed on TiO$_2$ particles (20− 30 nm diameter).

The Pt/TiO$_2$ powder was redispersed in distilled water (0.5 g/L) under sonication, and then the ruthenium sensitizer was added. The typical sensitizer concentration added to the suspension was 10 μM. EDTA (10 mM) was added in the suspension as an electron donor to regenerate the oxidized sensitizers. The adsorption of each sensitizer on TiO$_2$ was measured as a function of pH both in the presence and absence of EDTA. The amount of the sensitizer adsorbed on TiO$_2$ was calculated from the absorbance difference (ΔA) between the initial sensitizer solution and the filtered solution of sensitizer-added suspension. At pH 3, all sensitizer molecules quantitatively adsorbed on TiO$_2$ in the absence of EDTA: the UV−vis absorption and emission

spectra showed no sign of sensitizers present in the filtrate (filtered through a 0.45-μm PTFE filter) of the equilibrated sensitizer-added TiO$_2$ suspension. Therefore, all hydrogen production experiments were carried out at pH 3, except for the case of pH-dependent investigation. Adsorbed sensitizers could be quantitatively desorbed from the TiO$_2$ surface at pH 11, and their concentration was compared before and after the photoreaction.

Photoreactivity Measurements. The visible light reactivities of the Pt/TiO$_2$/C- or P-complexes were tested for H$_2$ production. The light source was a 450-W Xe-arc lamp (Oriel) whose irradiation passed through a 10-cm IR water filter and a UV cutoff filter ($\lambda > 420$ nm) and then was focused onto a 30-mL reactor. The aqueous suspension containing the sensitized catalyst and EDTA (10 mM) at pH 3 was deaerated by N$_2$ sparging before irradiation, and the reactor was sealed from the ambient air during the irradiation. The production of H$_2$ was monitored using a HP6890A GC equipped with a TCD detector and a 5A molecular sieve column. Light intensity was measured through ferrioxalate actinometry as described elsewhere.[40] A typical incident light intensity was measured to be about 1.0 × 10^{-3} einstein L^{-1} min^{-1} in the wavelength range 420−500 nm.

Photoelectrochemical Measurements. The photoelectro-chemical characteristics of six RuL$_3$/TiO$_2$ electrodes immersed in water were measured so that the hydrogen production activity of RuL$_3$/TiO$_2$ particles in aqueous suspension could be com-pared. TiO$_2$ electrodes were prepared as described elsewhere.[41,42] Briefly, a paste made of TiO$_2$ powder and CARBOWAX (poly-(ethylene glycol)) binder in an ethanol/water mixture (1:2 v/v) was spread on a conducting glass (fluorine-doped SnO$_2$ glass, Pilkington, 1.65 cm^2) and distributed with a glass rod sliding over the tape-covered edges. After drying, the electrode was heated in an oven at 450 °C for 30 min in air to burn off organic binder. For the sensitization of the TiO$_2$ electrode, the electrode was immersed in an aqueous solution of ruthenium complexes (25 μM, pH 3.0) for 24 h. The resulting sensitized TiO$_2$ electrode was washed with distilled water (pH 3) and dried at room temperature. The photoelectrochemical cell was cylindrical and had a working electrode (C−TiO$_2$ or P−TiO$_2$), a reference saturated calomel electrode (SCE), and a counter graphite rod. The electrolyte used was 10 mM EDTA at pH 3. The photoelectrochemical response was measured by a potentiostat (EG&G, Model 263A) that was connected to a computer.

Results and Discussion

Sensitizer Adsorption and pH Effect Depending on the Anchoring Group. Figure 1 shows the pH-dependent adsorption of C-complexes in the absence (Figure 1a) and the presence (Figure 1b) of EDTA in aqueous suspension of TiO$_2$. As previously reported,[36] **C4** and **C6** are effectively adsorbed at pH <6, whereas **C2** shows negligible adsorption over the whole pH region. The pH-dependent adsorption of the C-complexes (predominantly anions) is directly related with the surface charge of TiO$_2$ that changes with pH.[36] Since the sensitizer adsorption on TiO$_2$ surface is a prerequisite for the sensitized production of hydrogen, understanding the characteristics of the sensitizer adsorption is critically important for achieving a higher ef-ficiency of hydrogen production. Figure 1b shows that the presence of EDTA (electron donor used in this study) signifi-cantly hinders the adsorption of C-complexes on TiO$_2$. At pH 3, where **C4** and **C6** quantitatively adsorb on TiO$_2$ in the absence of EDTA, their adsorption on TiO$_2$ is drastically reduced to 10% or less in the presence of 10 mM EDTA. **C6** shows the highest surface binding affinity among C-complexes. EDTA
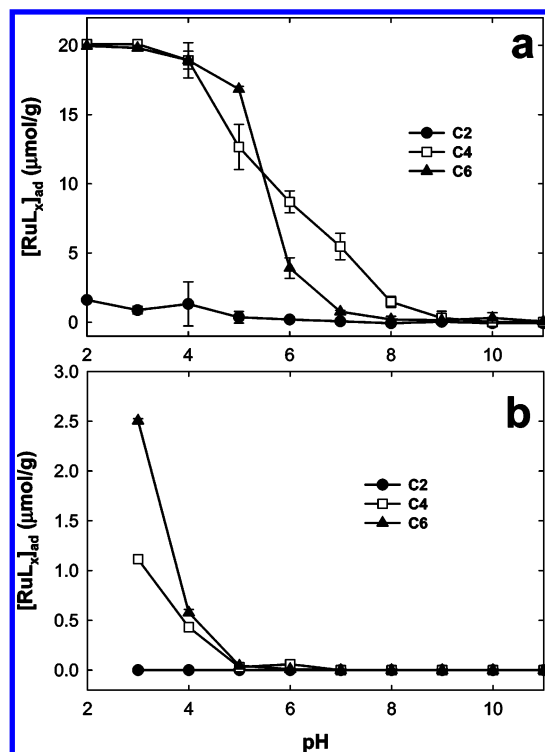

Figure 1. pH-dependent adsorption of C-complexes in the absence (a) and the presence (b) of EDTA in aqueous suspension of TiO$_2$. [TiO$_2$] = 0.5 g/L, [RuL$_x$]$_i$ = 10 μM, [EDTA] = 10 mM.

molecules are present as an anionic form and strongly compete for the positively charged surface sites with C-complexes. Since EDTA is present in large excess compared to the sensitizer (10 mM vs 10 μM), the sensitizer adsorption is inhibited. This implies that the C−TiO$_2$/EDTA system cannot be efficient. Although EDTA is the most efficient electron donor in this system, its presence limits the overall sensitization efficiency by blocking the adsorption of sensitizers. Using methanol instead of EDTA as an electron donor was very inefficient in producing hydrogen, although methanol is thought to be a much weaker adsorbate than EDTA.

On the other hand, the characteristics of the adsorption of P-complexes and the effect of EDTA are markedly different from those of C-complexes. Figure 2a shows that P-complexes were effectively adsorbed on TiO$_2$ over a wider range of pH than C-complexes. The detailed comparison between the adsorption behaviors of C- and P-complexes, which are highly dependent on the kind and number of anchoring groups, was previously discussed.[36] The most outstanding difference in the surface adsorption between C- and P-complexes is the interfering effect of EDTA. The addition of excess EDTA only moderately reduced the adsorption of P-complexes (Figure 2b), which is drastically contrasted with the case of C-complexes (Figure 1b). P-complexes with EDTA show nonnegligible adsorption up to pH 8, whereas the adsorption of C-complexes with EDTA is completely absent, even at pH 5. This indicates that the surface binding affinity of P-complexes is much stronger than that of EDTA and implies that P-complexes should be far better sensitizers for hydrogen production than C-complexes. All P-complexes show comparable surface affinity and the adsorp-tion of **P4** is most favored.

Figure 3 compares the pH-dependence of the hydrogen production between C−TiO$_2$ (Figure 3a) and P−TiO$_2$ (Figure 3b) systems. The profiles of the pH-dependent hydrogen production are qualitatively similar to those of the pH-dependent adsorption (with EDTA) that are shown in Figures 1b and 2b.
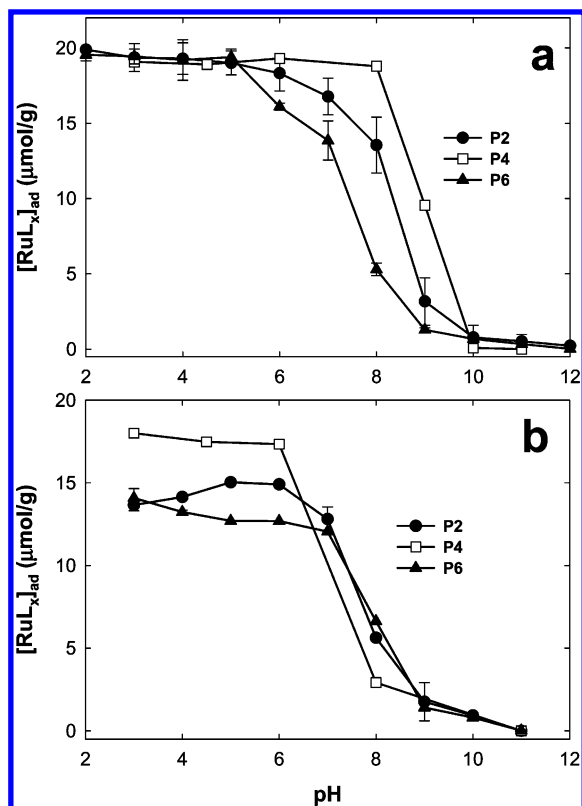
Effect of Anchor in Ru-Complex-Sensitized TiO2

J. Phys. Chem. B, Vol. 110, No. 30, 2006 **14795**

Figure 2. pH-dependent adsorption of P-complexes in the absence (a) and the presence (b) of EDTA in aqueous suspension of TiO2. [TiO2] = 0.5 g/L, $[RuL_x]_i$ = 10 μM, [EDTA] = 10 mM.
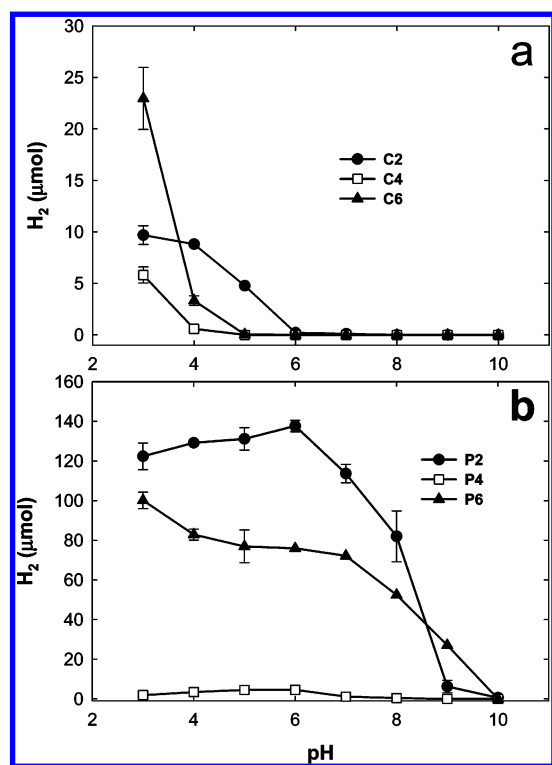

Figure 3. pH-dependent H2 production in (a) C−TiO2 and (b) P−TiO2 suspension under visible light irradiation. The experimental conditions were [TiO2] = 0.5 g/L, $[RuL_x]_i$ = 10 μM, [EDTA] = 10 mM, λ > 420 nm, 2-h irradiation, and initially N2-saturated.

As expected from the adsorption data, P−TiO2 is far more efficient than C−TiO2 in hydrogen production. While the hydrogen production with C−TiO2 is inefficient and limited
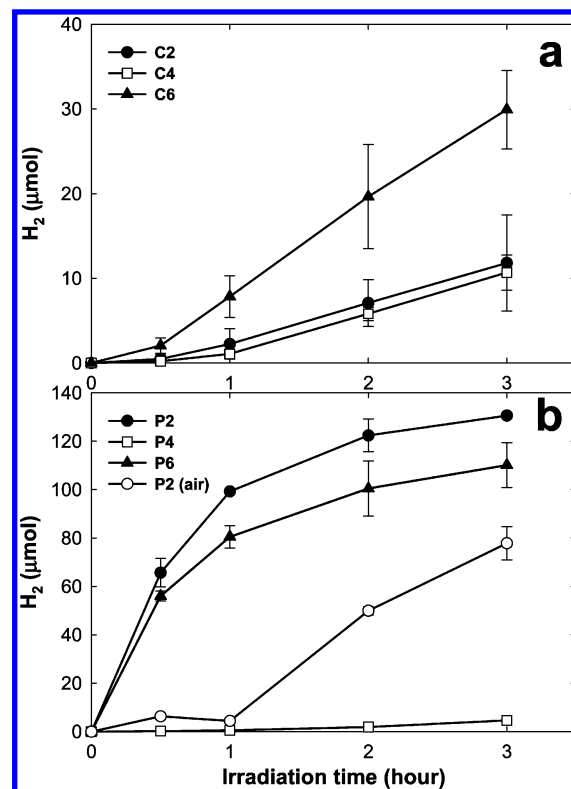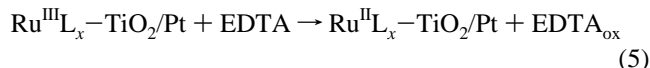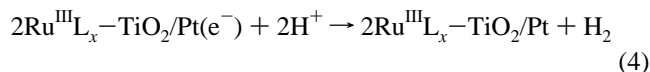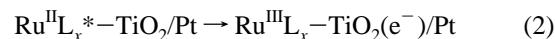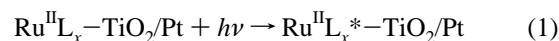

Figure 4. Time-dependent profiles of hydrogen production in the visible light-irradiated suspensions of (a) C−TiO2 and (b) P−TiO2. The hydrogen production with **P2**−TiO2 is compared between N2- and air-saturated conditions. The experimental conditions were [TiO2] = 0.5 g/L, pHi = 3, $[RuL_x]_i$ = 10 μM, [EDTA] = 10 mM, λ > 420 nm, and initially N2-saturated.

below pH 4, that in the P−TiO2 system is much higher and extended up to pH 9.

Sensitized Production of Hydrogen on C−TiO2 and P−TiO2. The sensitized production of hydrogen is based on the following reaction scheme.[5,22]

$$Ru^{II}L_x-TiO_2/Pt + h\nu \rightarrow Ru^{II}L_x^*-TiO_2/Pt \qquad (1)$$

$$Ru^{II}L_x^*-TiO_2/Pt \rightarrow Ru^{III}L_x-TiO_2(e^-)/Pt \qquad (2)$$

$$Ru^{III}L_x-TiO_2(e^-)/Pt \rightarrow Ru^{III}L_x-TiO_2/Pt(e^-) \qquad (3)$$

$$2Ru^{III}L_x-TiO_2/Pt(e^-) + 2H^+ \rightarrow 2Ru^{III}L_x-TiO_2/Pt + H_2 \qquad (4)$$

$$Ru^{III}L_x-TiO_2/Pt + EDTA \rightarrow Ru^{II}L_x-TiO_2/Pt + EDTA_{ox} \qquad (5)$$

Two molecules of ruthenium sensitizers are oxidized per one H2 molecule generated and they need to be regenerated successively by electron donors (reaction 5) to sustain the reactivity. Provided that EDTA is a one-electron donor, two molecules of EDTA should be consumed upon generating one H2 molecule as well. If the above reaction scheme were nonregenerative, the hydrogen production should be stoichiometric. That is, the hydrogen production should stop after generating only 0.13 μmol of H2 in this case, where the initial sensitizer added to the reactor was 0.25 μmol (10 μM × 25 mL). Figure 4 shows that the actual hydrogen production in both C−TiO2 and P−TiO2 suspensions goes far beyond this level, which indicates that the sequence of reactions 1−5 is cycling. The production of one H2 molecule requires two

reaction cycles. The most efficient case (**P2**−TiO₂) generated about 120 μmol of H₂ in 2 h (or 1 μmol/min), which corresponds to an average of eight reaction cycles per minute. The above sensitized production of hydrogen was carried out in the absence of dissolved oxygen, since O₂ is a competing electron acceptor with H⁺ (reaction 6).[21b]

When the photoirradiation was done in the air-saturated suspension of **P2**−TiO₂, the hydrogen production was markedly retarded (Figure 4b). Hydrogen started to evolve after 1-h irradiation, during which dissolved O₂ was depleted by reaction 6.

$$Ru^{III}L_x-TiO_2/Pt(e^-) + O_2 \rightarrow Ru^{III}L_x-TiO_2/Pt + O_2^{\cdot-} \quad (6)$$
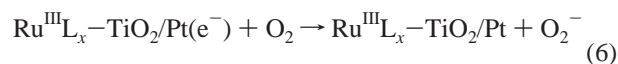
As for the pH change, two reactions are counteracting: the degradation of EDTA may generate protons, but the hydrogen production should consume them. Therefore, the net pH change was not significant. The pH slightly increased from 3.0 to 3.3− 3.4 after 3-h photoreaction in both C−TiO₂ and P−TiO₂ systems.

It should be noted that the time-dependent profiles of hydrogen production are very different between the C−TiO₂ and P−TiO₂ systems. Figure 4 shows that the evolution of hydrogen with C−TiO₂ requires an induction period of about 30 min, whereas the hydrogen evolution immediately followed the irradiation in P−TiO₂ suspension. The marked difference in the initial hydrogen production rate between C−TiO₂ and P−TiO₂ suspensions cannot be clearly explained but appears to be related with the different condition of adsorbed sensitizers. C-complexes are weakly adsorbed on TiO₂ that is fully covered with EDTA molecules. Under this condition, the formation of the carboxylate linkages between the TiO₂ surface and C-complexes, which is essential for the efficient electron injection, are not well developed and their sensitization action is inhibited in the initial period. It seems that C-complexes form the surface linkages during the induction period. On the other hand, the hydrogen production rate in P−TiO₂ suspension was initially high but gradually decelerated with irradiation time and then became similar to that of C−TiO₂ in 2-h irradiation. The gradual loss of activity of P−TiO₂ should not be ascribed to the depletion of electron donors (EDTA), since the addition of a fresh aliquot of EDTA to the reactor did not recover the activity. One possibility is that sensitizers were degraded on TiO₂ under visible light. In our previous study, it was observed that **P2** on TiO₂ was significantly degraded after 6-h visible irradiation in the absence of added electron donors.[22] To check out this possibility in the present case with electron donors (EDTA), the concentrations of sensitizers were compared before and after visible light irradiation by monitoring the change of their UV− visible absorption spectra. Adsorbed sensitizers could be quantitatively recovered from the TiO₂ surface by desorbing them at alkaline pH and filtering out TiO₂ particles. The degradation of some sensitizers was observed to some degree but was not large enough to explain the activity loss. After 6-h visible light irradiation, the concentration of **P6** decreased by 30%, but that of **P2** (the most active sensitizer) was not reduced at all. This indicates that **P2** sensitizers are continuously and quantitatively regenerated as long as EDTA is present, whereas the regeneration of **P6** is not complete. In any case, the loss of hydrogen production activity should not be due to the sensitizer degradation. Another factor that causes the cessation of H₂ production is that an equilibrium is achieved as hydrogen gas accumulates in the headspace of the photoreactor. The CB edge potential of TiO₂ and the H⁺/H₂ reduction potential are −0.28

TABLE 1: Initial Rates of Hydrogen Generation in the Aqueous Suspensions of Sensitized TiO₂ under Visible Light Irradiation[a]

TiO₂ (BET surface area, m²/g)	H₂ (μmol/min)	
	C6[b] (AQE, %)[c]	**P2** (AQE, %)[c]
Degussa P25 (50)	0.18 ± 0.02 (1.4)	2.2 ± 0.01 (17.6)
Hombikat UV100 (348)	1.14 ± 0.02 (9.1)	2.8 ± 0.2 (22.4)
Ishihara ST01 (340)	0.5 ± 0.1 (4.0)	3.5 ± 0.1 (28.0)
Aldrich anatase (9.2)	0 (0)	0.09 ± 0.04 (0.7)

[a] Experimental conditions: [TiO₂] = 0.5 g/L, pH_i = 3, [RuL_x]_i = 10 μM, [EDTA] = 10 mM, suspension volume 25 mL, λ > 420 nm, and initially N₂-saturated. [b] The initial rates were estimated after an induction period of 30 min. [c] Apparent quantum efficiency (AQE) = 2 × (H₂ generation rate)/(incident light intensity).

and −0.18 V (vs NHE) at pH 3, respectively. The CB electron initially has a moderate driving force for the production of hydrogen. However, the gradual accumulation of hydrogen gas in the closed reactor shifts $E(H^+/H_2)$ to the negative value and reduces the driving force until the equilibrium is reached with stopping the hydrogen production. When we repeated the cycles of hydrogen production after purging the reactor with N₂ gas, however, the initial hydrogen production rate could not be restored to the original value. Therefore, the most plausible explanation seems to be that the sensitizer−surface linkages are gradually broken down under irradiation (without the degradation of sensitizer itself), which subsequently undermines the sensitizing activity. Our previous FT-IR investigation showed that the sensitizer−surface linkages in **C6**−TiO₂ and **P2**−TiO₂ underwent a gradual hydrolytic cleavage even under the dark condition.[22]

It is also interesting to note that the sensitized production of hydrogen showed a strong dependence on the kind of TiO₂ supports. Table 1 compares the initial rates of hydrogen generation among the **C6**−TiO₂ and **P2**−TiO₂ systems that employed various commercial TiO₂ samples as a support under the otherwise identical experimental conditions. **C6** and **P2** were selected for comparison, since they were the most efficient sensitizers among the series. Four commercial TiO₂ samples (Degussa P25, Hombikat UV-100, Ishihara ST-01, and Aldrich anatase) were compared here. **P2**−TiO₂ exhibited consistently higher reactivities than **C6**−TiO₂, regardless of the kind of TiO₂ supports. Hombikat and Ishihara samples that have much higher surface area than Degussa were more efficient, although the added sensitizer concentration was the same. The Aldrich sample, which has a very low surface area, was inactive. The highly varying activity of sensitization among different TiO₂ supports might be related to various parameters, such as the total surface area of TiO₂, the density of the surface functional groups on TiO₂, the surface crystalline faces of TiO₂, and the morphology and dispersity of Pt cocatalyst.

Comparison with the Case of DSSC. The parallel comparison of the relative photoactivity of C- and P-complexes between the systems of DSSC (from ref 36) and the sensitized production of hydrogen (from this work) reveals that the efficiency of six sensitizers and the effect of the anchoring group are strikingly different between the two systems, which was hardly expected. **C4** was the most efficient sensitizer among C-complexes when they were compared for the performance of DSSC. In contrast to this, **C4** is the least efficient for the sensitized production of hydrogen among C-complexes according to the present result. In the case of DSSC, the **C4**−TiO₂ system showed the best cell performance, despite the lowest visible light absorption by **C4**, because the most effective surface binding mode is allowed

Effect of Anchor in Ru-Complex-Sensitized TiO$_2$

J. Phys. Chem. B, Vol. 110, No. 30, 2006 **14797**

with this structure. However, in the present situation, where excess EDTA strongly prohibits the adsorption of C-complexes on TiO$_2$, the subtle effect of the anchoring group on the surface binding mode becomes insignificant and the visible light absorption efficiency of C-complexes seems to control the overall activity. **C6** has the highest surface adsorption concentration in the presence of EDTA and the highest molar absorptivity in the visible region. The order in the sensitized hydrogen production (**C6** > **C2** > **C4**) follows the order in the MLCT band absorptivity. The adsorption of C-complexes on TiO$_2$ in the presence of excess EDTA should be of weak physical attraction, and their sensitizing capability is strongly limited, regardless of the number of carboxylate groups. The fact that **C2** shows higher activity for hydrogen production than **C4**, despite the complete absence of **C2** adsorbed on TiO$_2$, implies that the sensitizer−TiO$_2$ interaction is of physical nature and that the role of the surface chemical anchoring through the carboxylate group is less important in this case.

On the other hand, **P2** is the most active sensitizer for the hydrogen production. This is also contrasted with the case of DSSC, in which **P6** was the most efficient. The highest activity of **P6** among P-complexes tested for DSSC performance has been previously ascribed to its highest MLCT molar absorptivity, which is about double and triple that of **P2** and **P4**, respectively. The present observation that **P2** is a better sensitizer for hydrogen production than **P6** indicates that other factors should play a role. The most probable explanation appears to be related with the change in the surface charge. When the ζ-potentials were measured in the aqueous suspension of TiO$_2$, the addition of **P2** to the suspension had no influence on the surface potential, but the addition of 10 μM **P6** drastically reversed the surface potential from +30 to −12 mV at pH 3. Such a charge reversal might make the negatively charged electron donors (EDTA) less available at the surface site and hence reduce production of hydrogen. This is also consistent with the fact that **P6** was not quantitatively regenerated during irradiation, whereas **P2** was. On the other hand, the adsorption of **P4** is the most efficient in the presence of EDTA, but **P4** was almost completely inactive for hydrogen production, despite its strong surface affinity. The surprisingly low activity of **P4** is consistent with what we observed in the study of DSSC.[36] **P4** has the lowest visible light absorption (MLCT band) among P-complexes, but the complete inactivity cannot be explained by this alone. The fact that **P4** fails to function as a visible light sensitizer on TiO$_2$ both in DSSC (organic solvent-based system)[36] and in sensitized hydrogen production (aquatic system) implies that the poor sensitizing activity of **P4** is intrinsic in itself and should not be ascribed to the nature of the specific interfacial (sensitizer/support/solvent) environment.

Sensitizing Activities and Photocurrents in C−TiO$_2$ and P−TiO$_2$. The photocurrent generation profiles obtained with visible light sensitized TiO$_2$ electrodes (in the presence of EDTA) were compared with the sensitized hydrogen production in aqueous suspensions of C−TiO$_2$ and P−TiO$_2$. Figure 5 shows that the order in the magnitude of photocurrents obtained with the sensitized TiO$_2$ electrodes (at pH 3) follows the order in the hydrogen production obtained in the sensitized TiO$_2$ suspensions (at pH 3). The appearance of photocurrents indicates that electrons are injected from the adsorbed sensitizers to the TiO$_2$ electrode: higher photocurrents result from more electrons transferred. Therefore, the photocurrent and the hydrogen production are directly correlated, which is confirmed from the comparison between Figures 4 and 5. In accordance with the hydrogen production data (Figure 4), the photocurrents with
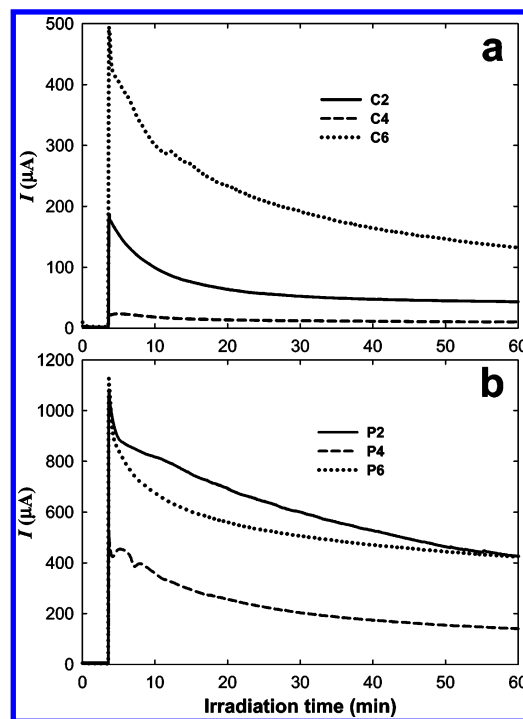

Figure 5. Visible light-induced photocurrent generation profiles obtained with the electrodes of (a) C−TiO$_2$ and (b) P−TiO$_2$ in 10 mM EDTA solution (pH 3) with an applied voltage of 0.5 V (vs SCE).

P−TiO$_2$ electrodes are consistently higher than C−TiO$_2$ electrodes. The fact that the photocurrent with **C4**−TiO$_2$ electrode is negligibly small is in marked contrast to our previous observation that the **C4**−TiO$_2$ electrode generated the highest photocurrent in DSSC among C−TiO$_2$ electrodes.[36] **P4**−TiO$_2$ exhibits the lowest hydrogen production and the smallest photocurrent, but the two quantities are not quantitatively proportional: the hydrogen production with **P4** is negligible, but the photocurrent obtained with **P4** is nonnegligible compared with that of **P2** and **P6**.

The effect of the sensitizer concentration on the sensitizing efficiency was compared for both the photocurrent and the hydrogen production. Since **C6** and **P2** exhibited the highest activity in each group of sensitizers, their sensitizing efficiency is investigated as a function of the sensitizer concentration, as shown in Figures 6 (**C6**) and 7 (**P2**). For both **C6** and **P2**, the concentration-dependent profile of photocurrent is very similar to that of hydrogen production. This suggests that the simple photocurrent measurement can be used as an indicator for the activity of sensitized photocatalysts. While the photocurrent and hydrogen production obtained with **C6**−TiO$_2$ showed a maximum at [**C6**] = 10 μM, those of **P2**−TiO$_2$ monotonically increased with the sensitizer concentration. In general, higher sensitization efficiency is expected at higher surface concentration of sensitizers. The fact that the sensitization efficiency of **C6**−TiO$_2$ is reduced at [**C6**] > 10 μM while **P6**−TiO$_2$ is not seems to be related to the unique adsorption behavior of **C6** on the TiO$_2$ surface. In the previous study, we suggested that the lower efficiency of **C6** as a sensitizer in DSSC be ascribed to the agglomerating nature of the **C6** molecules.[36] It seems that **C6** tends to form aggregates that do not adsorb uniformly on the surface of TiO$_2$ when its concentration is higher than 10 μM. Agglomerated dyes would be inefficient in electron injection.

Figure 8 shows the effect of the electron donor (EDTA) concentration on the sensitized production of hydrogen with **C6**−TiO$_2$ and **P2**−TiO$_2$. The EDTA-concentration-dependent
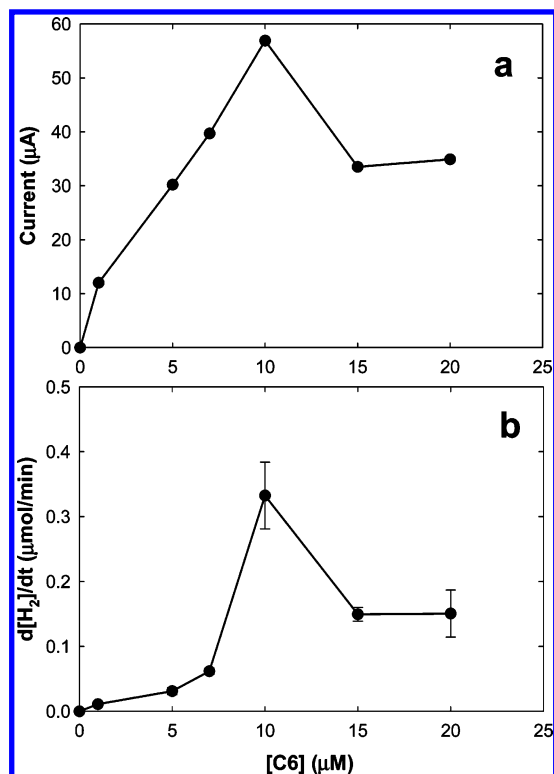
Figure 6. (a) Initial photocurrents obtained with **C6**−TiO$_2$ electrode in EDTA solution and (b) initial hydrogen production rates obtained in **C6**−TiO$_2$ suspension as a function of **C6** concentration. The experimental conditions were the same as those of Figure 4.
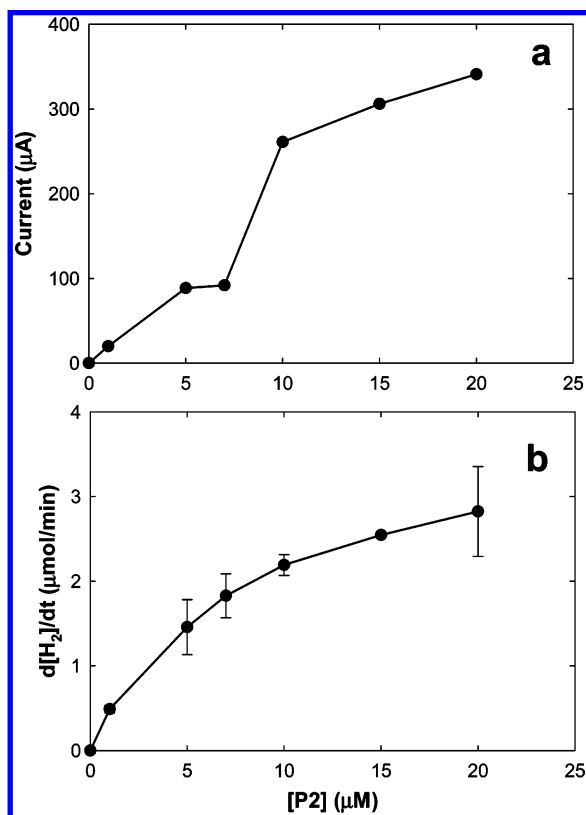

Figure 7. (a) Initial photocurrents obtained with **P2**−TiO$_2$ electrode in EDTA solution and (b) initial hydrogen production rates obtained in **P2**−TiO$_2$ suspension as a function of **P2** concentration. The experimental conditions were the same as those of Figure 4.

profiles are qualitatively very similar to the sensitizer-concentration-dependent profiles that are shown in Figures 6 and 7. **C6**−
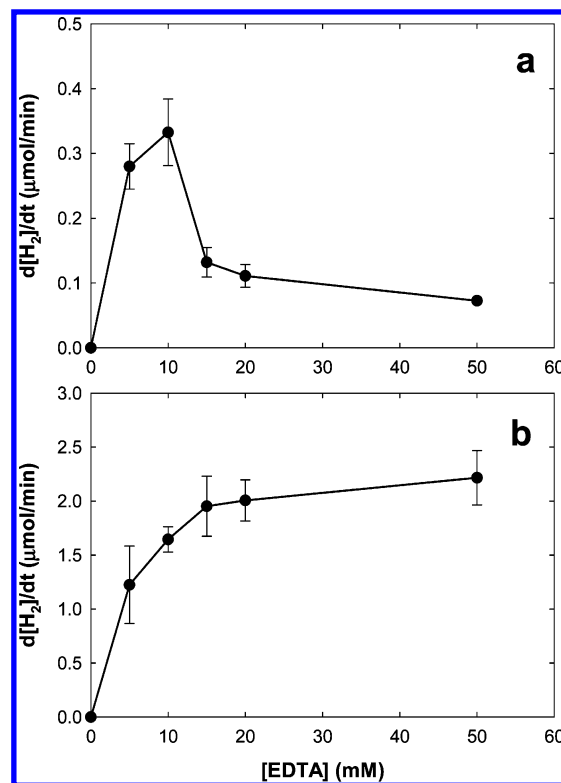

Figure 8. Initial hydrogen production rates as a function of EDTA concentration in (a) **C6**−TiO$_2$ and (b) **P2**−TiO$_2$ suspension. The experimental conditions were the same as those of Figure 4.

TiO$_2$ showed a maximum activity at [EDTA] = 10 mM, but **P2**−TiO$_2$ did not. As discussed with the adsorption data, the presence of excess EDTA strongly inhibited the adsorption of C-complexes but not that of P-complexes. Therefore, the addition of EDTA beyond an optimal concentration level reduced the overall activity by suppressing the adsorption of C-complexes even more, but it little affected the activity in the P−TiO$_2$ system because of the intrinsically stronger bonding between the P-complexes and TiO$_2$ surface.

Conclusions

We have systematically investigated the effects of the anchoring groups in ruthenium bipyridyl complexes on the sensitized production of hydrogen in an aqueous suspension of TiO$_2$ that was used as a support of the sensitizers. Six ruthenium-complex sensitizers having carboxylate (C-complex) or phosphonate (P-complex) anchoring groups were compared for their activity. The surface binding on TiO$_2$ and the sensitization efficiency depended on the anchoring group of the sensitizer, which behaved very differently between C- and P-complexes. Although the visible light absorbing capabilities among C- and P-complexes are comparable, P-complexes are much better sensitizers for hydrogen production because of the stronger surface anchoring of P-complex on TiO$_2$. The adsorption of P-complexes on TiO$_2$ is strong enough not to be hampered by the presence of competing adsorbates (EDTA), whereas that of C-complexes is significantly inhibited. Among P-complexes, **P2** was the most active and the most stable under visible light irradiation. The time-dependent profiles of hydrogen production and the effects of sensitizer and electron donor concentration on the hydrogen production activity were all very different between C−TiO$_2$ and P−TiO$_2$ systems.

We recently carried out a similar study that investigated the anchoring group effect on the photovoltaic behavior of DSSC

Effect of Anchor in Ru-Complex-Sensitized TiO₂

J. Phys. Chem. B, Vol. 110, No. 30, 2006 **14799**

for the same set of six sensitizers.[36] Since the basic principle of sensitization in both the sensitized TiO₂ electrode (DSSC) and the sensitized production of hydrogen on TiO₂ is the same, one may expect to see similar behaviors (or anchoring group effect) between the two systems. The outcome is quite contrary to the expectation: the effects of the anchoring group are strikingly different between the two systems. This is because the interfacial (TiO₂/sensitizer/medium) environment is very different in many aspects (e.g., solvent, electrolyte, surface charge), although the same sensitizers were compared.

The anchoring group effects on the sensitization of TiO₂ are primarily related with the formation of surface chemical bonds, but they are influenced by many other indirect factors, as revealed in this study and the previous one.[36] By changing the kind and the number of anchoring groups, not only the intrinsic properties of the surface chemical bonds but also the visible light absorbing capability and the surface charge are affected. The anchoring group effects are also related with the kind of solvent and the presence of competing adsorbates, such as electron donors and electrolytes.

Supporting Information Available: UV−vis absorption and emission spectra of six ruthenium bipyridyl sensitizers (PDF). This material is available free of charge via the Internet at http://pubs.acs.org.

References and Notes

(1) Fujishima, A.; Honda, K. *Nature* **1972**, *238*, 37.

(2) *Photocatalysis-Fundamentals and Applications;* Serpone, N., Pelizzetti, E., Eds.; Wiley-Interscience: New York, 1989.

(3) Kim, H. G.; Hwang, D. W.; Kim, J.; Kim, Y. G.; Lee, J. S. *Chem. Commun.* **1999**, 1077.

(4) Abe, R.; Hara, K.; Sayama, K.; Domen, K.; Arakawa, H. *J. Photochem. Photobiol. A: Chem.* **2000**, *137*, 63.

(5) Furlong, D. N.; Wells, D.; Sasse, W. H. F. *J. Phys. Chem.* **1986**, *90*, 1107.

(6) Dhanalakshmi, K. B.; Latha, S.; Anandan, S.; Maruthamuthu, P. *Int. J. Hydrogen Energy* **2001**, *26*, 669.

(7) Abe, R.; Sayama, K.; Arakawa, H. *J. Photochem. Photobiol. A* **2004**, *166*, 115.

(8) Kim, H. G.; Borse, P. H.; Choi, W.; Lee, J. S. *Angew. Chem., Int. Ed.* **2005**, *44*, 4585.

(9) Maeda, K.; Teramura, K.; Lu, D.; Takata, T.; Saito, N.; Inoue, Y.; Domen, K. *Nature* **2006**, *440*, 295.

(10) Choi, W.; Termin, A.; Hoffmann, M. R. *J. Phys. Chem.* **1994**, *98*, 13669.

(11) Asahi, R.; Morikawa, T.; Ohwaki, T.; Aoki, K.; Taga, Y. *Science* **2001**, *293*, 269.

(12) Sakthivel, S.; Kisch, H. *Angew. Chem., Int. Ed.* **2003**, *42*, 4908.

(13) Fessenden, R. W.; Kamat, P. V. *J. Phys. Chem.* **1995**, *99*, 12902.

(14) Hagfelt, A.; Grätzel, M. *Chem. Rev.* **1995**, *95*, 49.

(15) Stipkala, J. M.; Castellano, F. N.; Heimer, T. A.; Kelly, C. A.; Livi, K. J. T.; Meyer, G. J. *Chem. Mater.* **1997**, *9*, 2341.

(16) Hara, M.; Nunoshige, J.; Takata, T.; Kondo, J. N.; Domen, K. *Chem. Commun.* **2003**, 3000.

(17) Liu, M.; You, W.; Lei, Z.; Zhou, G.; Yang, J.; Wu, G.; Ma, G.; Luan, G.; Takata, T.; Hara, M.; Domen, K.; Li, C. *Chem. Commun.* **2004**, 2192.

(18) Niishiro, R.; Kato, H.; Kudo, A. *Phys. Chem. Chem. Phys.* **2005**, *7*, 2241.

(19) Lobedank, J.; Bellmann, E.; Bendig, J. *J. Photochem. Photobiol. A* **1997**, *108*, 89.

(20) Abe, R.; Sayama, K.; Arakawa, H. *Chem. Phys. Lett.* **2002**, *362*, 441.

(21) (a) Cho, Y.; Choi, W.; Lee, C.-H.; Hyeon, T.; Lee, H.-I. *Environ. Sci. Technol.* **2001**, *35*, 966. (b) Bae, E.; Choi, W. *Environ. Sci. Technol.* **2003**, *37*, 147.

(22) Bae, E.; Choi, W.; Park, J.; Shin, H. S.; Kim, S. B.; Lee, J. S. *J. Phys. Chem. B* **2004**, *108*, 14093.

(23) Bauer, C.; Jacques, P.; Kalt, A. *J. Photochem. Photobiol. A* **2001**, *140*, 87.

(24) Chatterjee, D.; Dasgupta, S. *J. Photochem. Photobiol. C* **2005**, *6*, 186.

(25) O'Regan, B.; Grätzel, M. *Nature* **1991**, *353*, 737.

(26) Kalyanasundaram, K.; Grätzel, M. *Coord. Chem. Rev.* **1998**, *77*, 347.

(27) Grätzel, M. *Nature* **2001**, *414*, 338.

(28) Anderson, N. A.; Lian, T. *Annu. Rev. Phys. Chem.* **2005**, *56*, 491.

(29) Sauve, G.; Cass, M. E.; Coia, G.; Doig, S. J.; Lauermann, I.; Pomykal, K. E.; Lewis, N. S. *J. Phys. Chem. B* **2000**, *104*, 6821.

(30) Péchy, P.; Rotzinger, F. P.; Nazeeruddin, M. K.; Kohle, O.; Zakeeruddin, S. M.; Humphry-Baker, R.; Grätzel, M. *J. Chem. Soc., Chem. Commun.* **1995**, 65.

(31) Trammell, S. A.; Moss, J. A.; Yang, J. C.; Nakhle, B. M.; Slate, C. A.; Odobel, F.; Sykora, M.; Erickson, B. W.; Meyer, T. J. *Inorg. Chem.* **1999**, *38*, 3665.

(32) Montalti, M.; Wadhwa, S.; Kim, W. Y.; Kipp, R. A.; Schmehl, R. H. *Inorg. Chem.* **2000**, *39*, 76.

(33) Gillaizeau-Gauthier, I.; Odobel, F.; Alebbi, M.; Argazzi, R.; Costa, E.; Bignozzi, C. A.; Qu, P.; Meyer, G. J. *Inorg. Chem.* **2001**, *40*, 6073.

(34) Merrins, A.; Kleverlaan, C.; Will, G.; Rao, S. N.; Scandola, F.; Fitzmaurice, D. *J. Phys. Chem. B* **2001**, *105*, 2998.

(35) Qu, P.; Meyer, G. J. *Langmuir* **2001**, *17*, 6720.

(36) Park, H.; Bae, E.; Lee, J.-J.; Park, J.; Choi, W. *J. Phys. Chem. B* **2006**, *110*, 8740.

(37) Nazeeruddin, M. K.; Zakeeruddin, S. M.; Humphry-Baker, R.; Jirousek, M. L., P.; Vlachopoulos, N.; Shklover, V.; Fischer, C. H.; M., G. *Inorg. Chem.* **1999**, *38*, 6298.

(38) Penicaud, V.; Odobel, F.; Bujoli, B. *Tetrahedron Lett.* **1998**, *39*, 3689.

(39) Zabri, H.; Gillaizeau, I.; Bignozzi, C. A.; Caramori, S.; Charlot, M.-F.; Cano-Boquera, J.; Odobel, F. *Inorg. Chem.* **2003**, *42*, 6655.

(40) Hatchard, C. G.; Parker, C. A. *Proc. R. Soc. London. Ser. A* **1956**, *235*, 518.

(41) Park, H.; Kim, K. Y.; Choi, W. *J. Phys. Chem. B* **2002**, *106*, 4775.

(42) Mills, A.; Elliott, N.; Hill, G.; Fallis, D.; Durrant, J. R.; Wills, R. L. *Photochem. Photobiol. Sci.* **2003**, *2*, 591.